HHS Public Access

Author manuscript

Epilepsy J. Author manuscript; available in PMC 2018 November 14.

Published in final edited form as:

Epilepsy J. 2018 ; 4(2): . doi:10.4172/2472-0895.1000128.

Characterizing Concentration-Dependent Neural Dynamics of 4-Aminopyridine-Induced Epileptiform Activity

Timothy L Myers[1,2], **Oscar C Gonzalez**[3,4], **Jacob B Stein**[2], and **Maxim Bazhenov**[3,*]

[1]Neuroscience Graduate Program, University of California, Riverside, California, United States of America

[2]Department of Cell Biology and Neuroscience, University of California, Riverside, California, United States of America

[3]Department of Medicine, University of California, San Diego, California, United States of America

[4]Neuroscience Graduate Program, University of California, San Diego, California, United States of America

Abstract

Epilepsy remains one of the most common neurological disorders. In patients, it is characterized by unprovoked, spontaneous, and recurrent seizures or ictal events. Typically, inter-ictal events or large bouts of population level activity can be measured between seizures and are generally asymptomatic. Decades of research have focused on understanding the mechanisms leading to the development of seizure-like activity using various pro-convulsive pharmacological agents, including 4-aimnopyridine (4AP).

However, the lack of consistency in the concentrations used for studying 4AP-induced epileptiform activity in animal models may give rise to differences in results and interpretation thereof. Indeed, the range of 4AP concentration in both *in vivo* and *in vitro* studies varies from 3 μM to 40 mM. Here, we explored the effects of various 4AP concentrations on the development and characteristics of hippocampal epileptiform activity in acute mouse brain slices of either sex. Using multi-electrode array recordings, we show that 4AP induces hippocampal epileptiform activity for a broad range of concentrations.

The frequency component and the spatiotemporal patterns of the epileptiform activity revealed a dose-dependent response. Finally, in the presence of 4AP, reduction of KCC2 co-transporter activity by KCC2 antagonist VU0240551 prevented the manifestation of the frequency component differences between different concentrations of 4AP. Overall, the study predicts that different concentrations of 4AP can result in the different mechanisms behind hippocampal epileptiform activity, of which some are dependent on the KCC2 co-transporter function.

*Corresponding author: Bazhenov M, Department of Medicine, University of California, San Diego, California, United States of America, Tel: 858.534-8391; mbazhenov@ucsd.edu.

Keywords

4-aminopyridine; KCC2 co-transporter; Epileptiform activity; *in vitro* brain slices

Introduction

Potassium (K^+) channel activation has been shown to be responsible for the repolarization of the membrane potential following the depolarization phase of an action potential [1-5]. Differences in the type of K^+-channels expressed in a given neuron influence the properties of action potentials produced by the neuron [1,4]. Outward going K^+ A-type currents (I_A) have been shown to regulate the action potential firing rate by modulating the inter-spike interval in response to sub-threshold current injections [2-5]. The I_A is mediated by multimeric channels comprised of mainly Kv4 family α-subunits in combination with modulatory β-subunits [6]. Functional knock-out, through expression of dominant negative Kv4.2 α-subunits (Kv4.2DN) in rat cortical pyramidal neurons has been shown to selectively eliminate I_A, resulting in reduced action potential threshold, increased action potential duration, and increased neuronal excitability [5]. Additionally, experiments in rat hippocampal neurons have shown that nearly all of the K^+ current underlying the repolarization phase of an action potential can be accounted for by the I_A and the dendrotoxin-sensitive K^+ D-current (I_D) [3]. Due to its important role in regulating neuronal excitability, it is not surprising that the I_A has been the subject of intense study in its relation to epileptic seizures.

Certain genetic epilepsies have been linked to misregulated or mutated K^+ channels in humans [7-14]. Some patients suffering from intractable temporal lobe epilepsy have been shown to express Kv4 α-subunit mutations, specifically truncation mutations in Kv4.2 α-subunits [8,14]. In these patients, the mutation manifests as a reduction of the I_A thereby leading to hyperexcitability. Similarly, I_A and I_A antagonist 4-aminopyridine (4AP) has been shown to cause hyperexcitability and the development of seizure-like epileptiform discharges both *in vivo* and *in vitro* [15-23]. Recent work suggests that the mechanism by which 4AP induces epileptiform activity is not through its direct reduction of I_A or I_D and increased principle neuron excitation; rather, 4AP increases the excitability of both inhibitory and excitatory neurons, the former of which is pivotal in the development of seizure-like activity [15,17-19,21,23,24]. Previous studies have shown that the potassium-chloride co-transporter isoform 2 (KCC2) plays an important role in the generation of 4AP-induced seizure [15,17-19,22]. Indeed, in rat brain slices treated with 4AP, reduction of KCC2 activity prevents seizure-like discharges while inter-ictal activity remained relatively intact [18]. The mechanism and extent to which KCC2 influences the properties of 4AP-induced inter-ictal activity remains to be fully understood.

Previous studies have attempted to fill this gap in our understanding of the precise effects of 4AP on neuronal activity, but lack of consistency in their methodologies and concentrations of 4AP, ranging from 3 μM to 40 mM, used for such studies has prevented the development of a complete picture [18,20,21,23,25-28]. In our new study, we explored the concentration-dependent effects of 4AP on the spatiotemporal properties of induced epileptiform activity

in acute mouse hippocampal brain slices. We found that bath applied 4AP produced dose-specific epileptiform bursts, the properties of which depended on 4AP concentration. Additionally, the reduction of KCC2 co-transporter activity through bath applied VU0240551 prevented the generation of the higher frequency component of epileptiform bursts at high 4AP concentrations.

Materials and Methods

Animals

All experiments and procedures were performed according to University of California, Riverside Institutional Animal Care and Use Committee-approved protocols. Wild-type (Jackson Laboratory, C57BL/6J, stock number 000664) mice colonies were bred and maintained in house to generate pups for this study. All mice were provided fresh water and mouse chow ad libitum, and a consistent circadian cycle was maintained by the vivarium facility. Both male and female mice were used in this study.

Brain slice preparation

Postnatal day (P) 15-20 mice were anesthetized with isoflurane and quickly decapitated. The brain was rapidly removed and submerged in ice-cold, low $[Ca^{2+}]o$, high sucrose dissecting solution continuously oxygenated with carbogen (95%-5% O_2-CO_2) gas. Horizontal whole brain slices (300 μm) were made with a Leica 1200 S vibratome. Slices containing both hippocampus and entorhinal cortex were recovered in oxygenated normal artificial cerebrospinal fluid (ACSF) for 1 h at 32 C, and then stored at room temperature until use. The standard dissecting solution contained (mM): 87 NaCl, 2.5 KCl, 25 $NaHCO_3$, 1.25 NaH_2PO_4, 4 $MgCl_2$, 0.5 $CaCl_2$, 10 D-glucose, and 75 sucrose. During recordings, brain slices were continuously perfused with ACSF (3 ml/min flow rate) containing (mM): 125 NaCl, 2.5 KCl, 25 $NaHCO_3$, 1.25 NaH_2PO_4, 1 $MgCl_2$, 2 $CaCl_2$, 25 D-glucose, and 10 sucrose. Both solutions were maintained at pH 7.4 by continuous oxygenation with carbogen gas. All chemicals were obtained though Fisher Scientific unless otherwise specified.

Electrophysiological recordings

Multielectrode array (MEA) recordings were performed on a 60-channel perforated array (60pMEA200/30-Ti) with a low-noise amplifier (MEA1060-BC) from Multi Channel Systems. Hippocampal slices were prepared, as described above, placed on the array, and positioned such that the CA1, CA3, and dentate gyrus (DG) were centered over the recording electrodes. Channels with high noise level were silenced prior to recording. Experiments consisted of an initial 30 min ACSF control followed by eight consecutive 30 min conditions of increasing 4-aminopyridine concentrations (25-200 μM in 25 μM step sizes). To test the effect of the KCC2 co-transporter on the characteristics of 4AP-induced epileptiform activity, we followed the same procedure outlined above, but added 10 μM of the KCC2 co-transporter antagonist VU0240551 to the perfusate containing 4AP. All MEA recordings were performed at 32 C, which was sufficient to generate stable epileptiform activity. For 4AP only experiments n=4 slices from 4 different mice, and for 4AP +VU0240551 n=6 slices from 6 different mice.

Analysis

Data were acquired using MC Rack software (MultiChannel Systems) and exported to MATLAB (Math Works) for further processing. Data from all 60 MEA channels were collected at 25 kHz and downsampled offline to 5 kHz. Synchronized network activity or epileptiform bursts recorded by the MEA were detected using our previously described percentile-based method [29]. Briefly, a low (1.25 ± 0.75) and high (98.75 ± 0.75) percentile were used on unfiltered data from a single channel recording from each of the hippocampal subfields mentioned above. The low percentile was used for events with negative polarity, while the high percentile was used for events with positive polarity. The amplitude corresponding to the low or high percentile was used as a threshold for detecting the epileptiform bursts. Similar to [29], burst onset was defined as the moment when the LFP crossed the percentile-defined threshold. The bursts were extracted from all channels with 500 ms before and after burst onset, and a non-overlapping period of 1 s was used. Inter-event intervals were computed as the difference between timing of the peak of a given event and that of the event prior to it. Event frequency was computed as the inverse of the inter-event interval. Fourier transforms were performed on the unfiltered, downsampled data using Matlab function fft. We used a sliding window of size 60 s with a 30 s overlap to compute the mean power spectrum. The mean was computed across all resulting transform signals across all slices for each condition. Data are presented as mean +/− standard error (SEM).

Results

We induced epileptiform activity throughout the hippocampal cortex by bath application of 4-aminopyridine (4AP). Local field potentials (LFPs) were recorded from the hippocampal subfields CA1, CA3, and DG using a 60-channel MEA (Figure 1A). Control, ACSF only, recordings showed minimal multiunit activity (data not shown). Spontaneous epileptiform activity was not observed in control conditions. Bath applied 4AP at all concentrations tested in this study (25 μM-200 μM) resulted in a transition from quiescence to a seizure-like state characterized by stereotyped continuous epileptiform activity (Figure 1). Epileptiform activity was robust, and highly synchronized across all MEA electrodes (Figure 1B). Single channel recordings from CA1, CA3, and DG revealed a bias towards CA3 as the generator of the largest epileptiform activity (Figures 1C and 1E). Figure 1D shows all the extracted epileptiform bursts (see Methods) from a single channel in CA3 superimposed (black traces) with the average burst superimposed in red. This revealed that the events recorded from the same channel show similar temporal properties throughout the duration of the burst. The temporal similarities in burst progression were not constrained to recordings from CA3. Figure 1F shows heat maps of all bursts recorded in the same channels from CA1, CA3, and DG revealing stereotyped activity induced throughout the hippocampus by 4AP.

As shown in Figure 1, 100 μM 4AP resulted in stereotyped epileptiform activity. Since 4AP selectively blocks outward going K^+ A- and D-currents, we hypothesized that varying the concentration of 4AP may lead to differences in the properties of the resulting epileptiform activity. To test this, we varied the concentration of bath applied 4AP, ranging from 25 μM-200 μM in 25 μM step sizes. Epileptiform activity was reliably elicited for all 4AP concentrations from that range.

We first examined the differences in the spatiotemporal distribution of epileptiform bursts throughout the hippocampus. Figure 2 shows the propagation of a single epileptiform burst (such as, e.g., shown in Figure 1D), resulting from different concentrations of bath applied 4AP, throughout the hippocampus. For all concentrations, the initiation of epileptiform bursts occurred near the CA3 subfield before propagating to the rest of the hippocampus (Figure 2). These epileptiform bursts initiated with a positive electrical potential (source) within the areas of the proximal and distal dendrites, which was accompanied by a negative potential (sink) within stratum pyramidale. Similar findings have been reported for epileptiform activity induced through elevated extracellular K^+ concentration ($[K^+]_o$) [29]. This was then followed by a reversal of the polarity of the field potentials in their respective locations.

We observed a much wider spatial distribution of epileptiform activity for low concentrations (Figure 2A). As seen for 25 and 50 μM concentrations, the electrical activity recorded during the 50-100 ms frame showed electrical activity propagating from CA3 to CA1. As mentioned previously, the stratum pyramidale exhibited a negative LFP while the regions containing pyramidal cell dendrites exhibited a positive LFP during early and middle phases of the epileptiform burst, which reversed in time during the later phase of the event. Additionally, in low concentrations (25-50 μM) the negative potential recorded from stratum pyramidale remained for 200 ms before reversing polarity. Unlike the prolonged period of negative LFP for low concentrations of 4AP, concentrations ranging from 75-100 μM exhibited a slightly prolonged period of positive LFP within CA3 and DG (compare time frames 125-200 ms, 200-250 ms, and 250-300 ms for concentrations 25-125 μM of Figures 2A and 2B). For high concentrations of 4AP (150-200 μM), the spatial distribution of the epileptiform burst became more focal and short lived (Figure 2C). Indeed, little activity was observed following 100 ms after the initiation of the epileptiform burst. These data suggest that the extent of the reduction of A- and D-current activity may cause substantial differences in the dynamics of the epileptiform activity.

The differences in the spatiotemporal distributions of the epileptiform activity shown in Figure 2 could reflect underlying differences in the frequency components of the epileptiform bursts. To explore this, we computed power spectrums of the electrical signals generated by the hippocampal slice under the conditions of bath applied 4AP. We observed that low concentrations of 4AP, 25-50 μM, generated epileptiform bursts that were mainly characterized by low frequencies <5 Hz (Figure 3A). The activity generated with 75 μM 4AP showed a small increase in higher frequencies (around 7-15 Hz), a trend also observed in epileptiform bursts generated at 100 μM 4AP (Figure 3B). These higher frequencies became more prominent at higher concentrations, 125-200 μM (Figure 3C). Insets show an example of a single corresponding epileptiform burst for the concentration indicated showing increased burst complexity with increasing 4AP concentration. Interestingly, the low frequency component of the epileptiform bursts remained largely intact at high concentrations. These data, along with the previously described data (Figure 2), support our hypothesis that differentially impairing A- and D- current activity results in different epileptiform activity profiles.

Recent evidence has suggested that the potassium-chloride co-transporter isoform 2 (KCC2) may play a key role in the generation of 4AP-induced epileptiform activity [15,17-19,22]. We hypothesized that the reduction of KCC2 activity by KCC2 antagonist VU0240551 may reduce the complexity of epileptiform activity elicited at higher concentrations of 4AP, resulting in more stereotyped epileptiform activity across various 4AP concentrations.

To test this hypothesis, we bath applied the KCC2 specific antagonist VU0240551, and varied the bath applied 4AP concentrations. Similar to our previous experiment (Figure 1), we observed 4AP-induced epileptiform for all concentrations tested with CA3 exhibiting the largest amplitude epileptiform bursts. Low 4AP concentration conditions (25-50 μM), once again, produced epileptiform activity dominated by low frequency activity (Figure 4). Interestingly, increasing the 4AP concentrations from 75-200 μM did not lead to a power spectrum peak at higher frequencies as seen previously in conditions of normal functioning KCC2 (compare Figures 3B, 3C, 4B and 4C). Additionally, the epileptiform activity elicited in the presence of the KCC2 antagonist became stereotyped across 4AP concentrations (compare Figure 4 insets). These findings suggest that the high frequency component of the epileptiform activity for high 4AP concentrations may be dependent on the recruitment of KCC2-dependent mechanisms.

Since application of the KCC2 co-transporter antagonist resulted in overall low frequency epileptiform activity for all 4AP concentrations tested, we hypothesized that this trend may be reflected in the inter-arrival times of the epileptiform bursts. To this end, we computed the inter-event interval for different 4AP concentrations for both 4AP only and 4AP +VU0240551 conditions. As shown in Figure 5A, increasing 4AP concentrations resulted in shorter inter-event intervals for both conditions (i.e. with and without VU0240551). In agreement with our hypothesis, reduction of KCC2 activity increased inter-event intervals (compare Figure 5B red and black Lines)

For the condition of 4AP only, we observed higher event frequencies as compared to the condition of reduced KCC2 activity (Figure 5B). The largest differences in event frequency were observed for lower concentrations (compare Figure 5B red and black).

As the concentration of 4AP increased, the frequency of events observed in the 4AP +VU0240551 condition increased to levels similar to those seen in the 4AP-only condition. A summary of the concentration-dependent differences for both 4AP only and 4AP +VU0240551 conditions are presented in Tables 1 and 2, respectively.

Discussion

K^+-channels regulate the intrinsic excitability of neurons and maintain the repolarization phase of action potentials [1-6,30-32]. Specifically, the I_A and I_D seem to account for nearly all of the K^+-current during this repolarization phase in principal neurons [3]. Due to the roles of these two currents in the regulation of neuronal excitability, they have been the focus of decades of intense study with the hope of gaining a better understanding of the mechanisms leading to the development of epilepsy [8,13-15,20,26]. In this new study, we tested the hypothesis that the effect of I_A and I_D channel antagonist 4-aminopyridine (4AP)

is strongly concentration-dependent. Different 4AP concentrations are characterized by qualitatively different spatiotemporal patterns of epileptiform activity in acute mouse hippocampal brain slices. Our *in vitro* data suggests that the spatiotemporal propagation, underlying frequency components, and inter-event intervals of 4AP-induced epileptiform activity vary with concentration. Furthermore, high concentrations of 4AP lead to the appearance of the high frequency component in epileptiform bursts, which may be dependent on the activation of the KCC2 co-transporter.

We found that for all concentrations used in our study, epileptiform activity originated in the CA3 hippocampal subfield before propagating to CA1 and DG. This result is similar to previously reported findings that the CA3 region is the initiator of epileptiform activity induced by elevated K^+ [29,33]. The local architecture of the CA3 makes it a prime candidate for seizure generation. Indeed, the pyramidal neurons within the CA3 exhibit a high degree of recurrent connectivity [34]. The differences in the spatiotemporal patterns of epileptiform activity arise during the application of “transition” 4AP concentrations (75-100 μM) and more so at high concentrations (125-200 μM). Tow 4AP concentrations (25-50 μM) generate longer lasting epileptiform bursts as compared to those induced by transitional and high concentrations. This may be due to altered excitability of hippocampal pyramidal neurons in response to reduced I_A and I_D. Previous studies in cultured pyramidal neurons showed that the elimination of I_A, by expression of Kv-4.2 dominant negative mutant, resulted in increased neuronal excitability to low-amplitude current stimulation [5]. Interestingly, large-amplitude current injections generated transient spiking before the neuron ceased spiking activity [5]. This reduction of prolonged spiking as a result of I_A reduction may explain the reduced durations of epileptiform bursts seen in at higher 4AP concentrations.

One of the more prominent concentration-dependent features we observed was the change in the frequency components of the induced epileptiform activity. For low concentrations of 4AP (25-50 μM), the epileptiform activity was dominated by a low frequency component (~5 Hz). As the concentration was increased towards 200 μM an additional high frequency component (~10 Hz) appeared. These changes in frequency were accompanied by overall reduction in the inter-event interval and increases in the frequency of events. This, along with the other observed concentration-dependent differences may be due to the relative differences in 4AP sensitivity exhibited by I_A and I_D. I_D has been shown to be much more sensitive to 4AP as compared to I_A [3]. As such, it is likely that the I_D is selectively blocked at the low concentrations used in this study and is responsible for the low frequency epileptiform activity. As the 4AP concentration was increased, 4AP may also block the I_A, in addition to I_D. This effect may explain the interesting transition observed for 75-100 μM 4AP. Additional experiments are needed to determine the relative contributions of these two currents in the development of epileptiform activity.

Recent work has pointed to the role of the KCC2 co-transporter in the development of 4AP-induced seizure [15,17-19,22]. KCC2-dependent efflux and accumulation of extracellular K^+ may drive transitions to a seizure-state by initiating a positive feedback loop in which elevated K^+ leads to network depolarization, which in turn leads to further accumulation of extracellular K^+ [17,23,35-40]. Previous studies have shown that 4AP-induced ictal, seizure-

like activity can be abolished in response to reduced KCC2 co-transporter activity [18]. With this in mind, we tested whether reduction of KCC2 co-transporter activity could prevent the changes in epileptiform activity induced at high 4AP concentrations. Our results showed that the high frequency component of the epileptiform activity was abolished in response to KCC2 antagonist VU0240551. Additionally, the inter-event interval was increased at low concentrations, while the event frequency was reduced for lower 4AP concentrations in the presence of VU0240551 as compared to 4AP only.. These data may point to differences in the mechanisms by which I_A and I_D reduction leads to seizure generation, with the former involving KCC2-dependent K^+ efflux and accumulation.

Conclusion

In sum, our study revealed the complex effect of 4AP application, possibly involving several complimentary biophysical mechanisms dependent on both ionic currents and exchangers. It further suggests that the relative contribution of these mechanisms to epileptiform activity and the overall effect of 4AP application may vary with 4AP concentration.

Acknowledgements

This work was supported by the National Institute of Health grants (1 R01 NS104368 and 1 R01 NS081243) and NSF Graduate Research Fellowship Grant DGE-1326120 (to O.C.G.).

References

1. Bean BP (2007) The action potential in mammalian central neurons. Nat Rev Neurosci: 8 451–465. [PubMed: 17514198]
2. Carrasquillo Y, Burkhalter A, Nerbonne JM (2012) A-type K+ channels encoded by Kv4.2, Kv4.3 and Kv1.4 differentially regulate intrinsic excitability of cortical pyramidal neurons. J Physiol 590: 3877–3890. [PubMed: 22615428]
3. Mitterdorfer J, Bean BP (2002) Potassium currents during the action potential of hippocampal CA3 neurons. J Neurosci 22: 10106–10115. [PubMed: 12451111]
4. Pathak D, Guan D, Foehring RC (2016) Roles of specific Kv channel types in repolarization of the action potential in genetically identified subclasses of pyramidal neurons in mouse neocortex. J Neurophysiol 115: 2317–2329. [PubMed: 26864770]
5. Yuan W, Burkhalter A, Nerbonne JM (2005) Functional role of the fast transient outward K+ current IA in pyramidal neurons in (rat) primary visual cortex. J Neurosci 25: 9185–9194. [PubMed: 16207878]
6. Birnbaum SG, Varga AW, Yuan LL, Anderson AE, Sweatt JD, et al. (2004) Structure and function of Kv4-family transient potassium channels. Physiol Rev 84: 803–833. [PubMed: 15269337]
7. Barnwell LF, Lugo JN, Lee WL, Willis SE, Gertz SJ, et al. (2009) Kv4.2 knockout mice demonstrate increased susceptibility to convulsant stimulation. Epilepsia 50: 1741–1751. [PubMed: 19453702]
8. D'Adamo MC, Catacuzzeno L, Di Giovanni G, Franciolini F, Pessia M (2013) K(+) channelepsy: progress in the neurobiology of potassium channels and epilepsy. Front Cell Neurosci 7: 134. [PubMed: 24062639]
9. Dazzo E, Santulli L, Posar A, Fattouch J, Conti S, et al. (2015) Autosomal dominant lateral temporal epilepsy (ADLTE): novel structural and singlenucleotide LGI1 mutations in families with predominant visual auras. Epilepsy Res 110: 132–138. [PubMed: 25616465]
10. Lascano AM, Korff CM, Picard F (2016) Seizures and Epilepsies due to channelopathies and neurotransmitter receptor dysfunction: A Parallel between Genetic and Immune Aspects. Mol Syndromol 7: 197–209. [PubMed: 27781030]

11. Nobile C, Michelucci R, Andreazza S, Pasini E, Tosatto SC, et al. (2009) LGI1 mutations in autosomal dominant and sporadic lateral temporal epilepsy. Hum Mutat 30: 530–536. [PubMed: 19191227]
12. Ottman R, Winawer MR, Kalachikov S, Barker-Cummings C, Gilliam TC, et al. (2004) LGI1 mutations in autosomal dominant partial epilepsy with auditory features. Neurology 62: 1120–1126. [PubMed: 15079011]
13. Schulte U, Thumfart JO, Klocker N, Sailer CA, Bildl W, et al. (2006) The epilepsy-linked Lgi1 protein assembles into presynaptic Kv1 channels and inhibits inactivation by Kvbeta1. Neuron 49: 697–706. [PubMed: 16504945]
14. Singh B, Ogiwara I, Kaneda M, Tokonami N, Mazaki E, et al. (2006) A Kv4.2 truncation mutation in a patient with temporal lobe epilepsy. Neurobiol Dis 24: 245–253. [PubMed: 16934482]
15. Avoli M, de Curtis M, Gnatkovsky V, Gotman J, Kohling R, et al. (2016) Specific imbalance of excitatory/inhibitory signaling establishes seizure onset pattern in temporal lobe epilepsy. J Neurophysiol 115: 3229–3237. [PubMed: 27075542]
16. de Curtis M, Avoli M (2016) GABAergic networks jump-start focal seizures. Epilepsia 57: 679–687. [PubMed: 27061793]
17. Gonzalez OC, Shiri Z, Krishnan GP, Myers TL, Williams S, et al. (2017) Role of KCC2-dependent potassium efflux in 4-Aminopyridine-induced Epileptiform synchronization. Neurobiol Dis 109:137–147. [PubMed: 29045814]
18. Hamidi S, Avoli M (2015) KCC2 function modulates in vitro ictogenesis. Neurobiol Dis 79: 51–58. [PubMed: 25926348]
19. Levesque M, Herrington R, Hamidi S, Avoli M (2016) Interneurons spark seizure-like activity in the entorhinal cortex. Neurobiol Dis 87: 91–101. [PubMed: 26721318]
20. Levesque M, Salami P, Behr C, Avoli M (2013) Temporal lobe epileptiform activity following systemic administration of 4-aminopyridine in rats. Epilepsia 54: 596–604. [PubMed: 23521339]
21. Shiri Z, Manseau F, Levesque M, Williams S, Avoli M (2016) Activation of specific neuronal networks leads to different seizure onset types. Ann Neurol 79: 354–365. [PubMed: 26605509]
22. Viitanen T, Ruusuvuori E, Kaila K, Voipio J (2010) The K+-CI cotransporter KCC2 promotes GABAergic excitation in the mature rat hippocampus. J Physiol 588: 1527–1540. [PubMed: 20211979]
23. Yekhlef L, Breschi GL, Lagostena L, Russo G, Taverna S (2015) Selective activation of parvalbumin- or somatostatin-expressing interneurons triggers epileptic seizurelike activity in mouse medial entorhinal cortex. J Neurophysiol 113: 1616–1630. [PubMed: 25505119]
24. Uva L, Breschi GL, Gnatkovsky V, Taverna S, de Curtis M (2015) Synchronous inhibitory potentials precede seizure-like events in acute models of focal limbic seizures. J Neurosci 35: 3048–3055. [PubMed: 25698742]
25. Ahn S, Jun SB, Lee HW, Lee S (2016) Computational modeling of epileptiform activities in medial temporal lobe epilepsy combined with in vitro experiments. J Comput Neurosci 41:207–223. [PubMed: 27416961]
26. Galvan M, Grafe P, ten Bruggencate G (1982) Convulsant actions of 4-aminopyridine on the guinea-pig olfactory cortex slice. Brain Res 241: 75–86. [PubMed: 7104708]
27. Guo ZS, Feng ZY, Yu Y, Zhou WJ, Wang ZX, et al. (2016) Sinusoidal stimulation trains suppress epileptiform spikes induced by 4-AP in the Rat Hippocampal CA1 REgion in vivo. In: Patton J, Barbieri R, Ji J, Jabbari E, Dokos S, et al. (eds) 2016 38th Annual International Conference of the Ieee Engineering in Medicine and Biology Society. IEEE Engineering in Medicine and Biology Society Conference Proceedings New York: 5817–5820.
28. Yu PN, Hsiao MC, Song D, Liu CY, Heck CN, et al. (2014) Unstable periodic orbits in human epileptic hippocampal slices. 2014 36th Annual International Conference of the Ieee Engineering in Medicine and Biology Society. IEEE Engineering in Medicine and Biology Society Conference Proceedings New York: 5800–5803.
29. Krishnan GP, Filatov G, Bazhenov M (2013) Dynamics of high-frequency synchronization during seizures. J Neurophysiol 109: 2423–2437. [PubMed: 23427308]

30. Cudmore RH, Fronzaroli-Molinieres L, Giraud P, Debanne D (2010) Spike-time precision and network synchrony are controlled by the homeostatic regulation of the D-type potassium current. J Neurosci 30: 12885–12895. [PubMed: 20861392]
31. Hyun JH, Eom K, Lee KH, Ho WK, Lee SH (2013) Activity-dependent downregulation of D-type K+ channel subunit Kv1.2 in rat hippocampal CA3 pyramidal neurons. J Physiol 591: 5525–5540. [PubMed: 23981714]
32. Metz AE, Spruston N, Martina M (2007) Dendritic D-type potassium currents inhibit the spike afterdepolarization in rat hippocampal CA1 pyramidal neurons. J Physiol 581: 175–187. [PubMed: 17317746]
33. Filatov G, Krishnan GP, Rulkov NF, Bazhenov M (2011) Dynamics of epileptiform activity in mouse hippocampal slices. J Biol Phys 37: 347–360. [PubMed: 21826119]
34. Le Duigou C, Simonnet J, Telenczuk MT, Fricker D, Miles R (2014) Recurrent synapses and circuits in the CA3 region of the hippocampus: an associative network. Front Cell Neurosci 7: 262. [PubMed: 24409118]
35. Bazhenov M, Timofeev I, Steriade M, Sejnowski TJ (2004) Potassium model for slow (2–3 Hz) in vivo neocortical paroxysmal oscillations. J Neurophysiol 92: 1116–1132. [PubMed: 15056684]
36. Frohlich F, Bazhenov M (2006) Coexistence of tonic firing and bursting in cortical neurons. Phys Rev E Stat Nonlin Soft Matter Phys 74: 031922. [PubMed: 17025682]
37. Gonzalez OC, Krishnan GP, Chauvette S, Timofeev I, Sejnowski T, et al. (2015) Modeling of age-dependent Epileptogenesis by differential homeostatic synaptic scaling. J Neurosci 35: 13448–13462. [PubMed: 26424890]
38. Krishnan GP, Bazhenov M (2011) Ionic dynamics mediate spontaneous termination of seizures and postictal depression state. J Neurosci 31: 8870–8882. [PubMed: 21677171]
39. Somjen GG (2002) Ion regulation in the brain: Implications for pathophysiology. Neuroscientist 8: 254–267. [PubMed: 12061505]
40. Wei Y, Ullah G, Schiff SJ (2014) Unification of neuronal spikes, seizures, and spreading depression. J Neurosci 34: 11733–11743. [PubMed: 25164668]

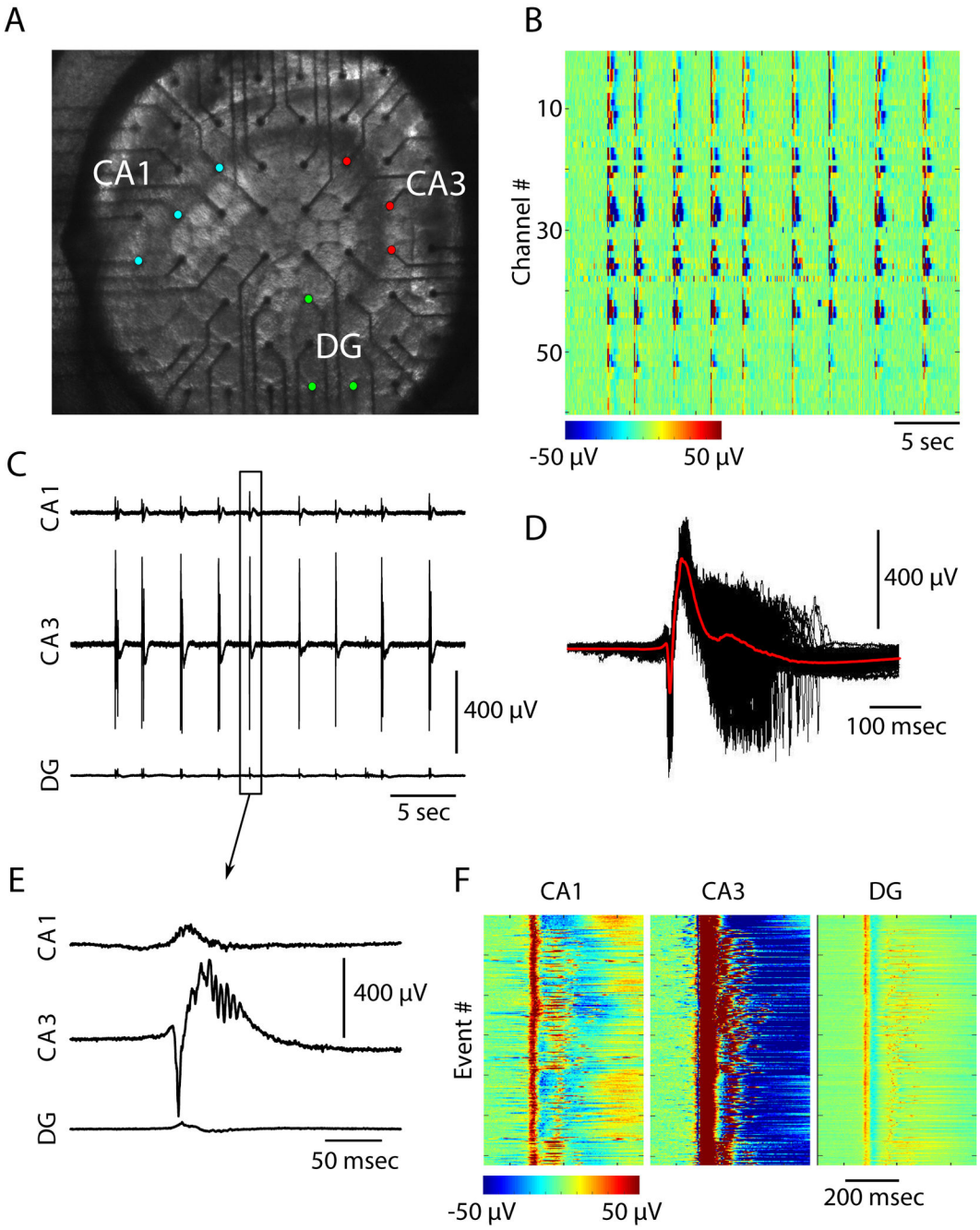

Figure 1: 4AP elicits epileptiform activity across the mouse hippocampus.

(A) Image showing the position of an acute mouse hippocampal brain slice on the multi-electrode array (MEA). CA1, CA3, and dentate gyrus (DG) subfields have been labeled, and colored electrodes correspond to electrodes within the structures **(B)** Epileptiform activity induced with 100 µM 4AP recorded by 60 channel MEA. Color scale represents voltage as indicated by scale bar **(C)** Epileptiform bursts recorded from single channels within the CA1 (top), CA3 (middle), and DG (bottom) **(D)** Time aligned epileptiform bursts recorded from a single CA3 electrode (black traces). The average signal is superimposed in red **(E)** Zoom in on a single burst from C **(F)** All epileptiform bursts recorded from the same channels in C.

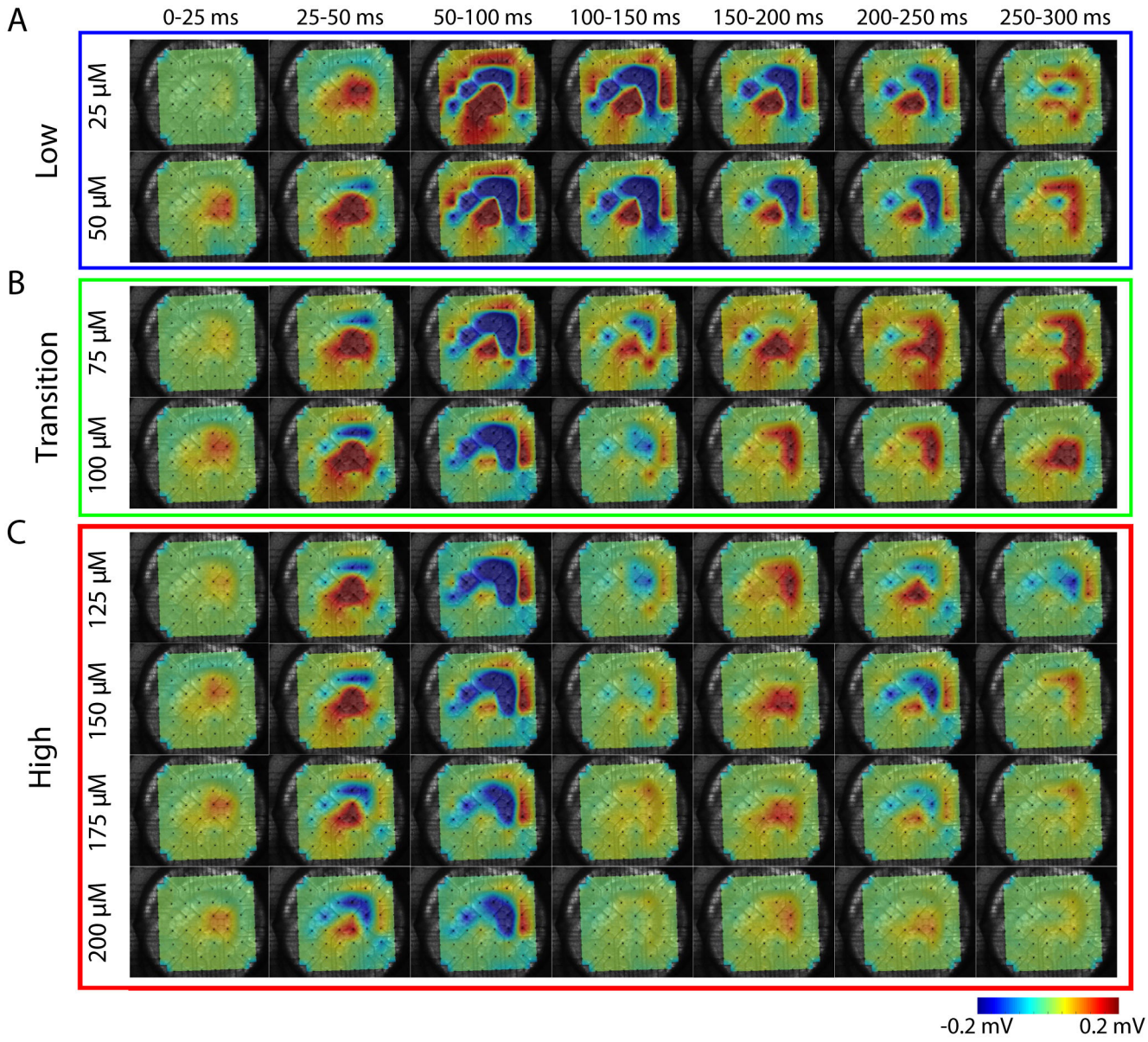

Figure 2: Concentration-dependent differences in spatiotemporal propagation of epileptiform activity.

Sequence of averaged (25 ms) LFP activity for one epileptiform burst. Each row corresponds to a different 4AP concentration **(A)** Low 4AP concentrations **(B)** Transition concentrations **(C)** High concentrations. Color represents voltage as indicated by the scale bar.

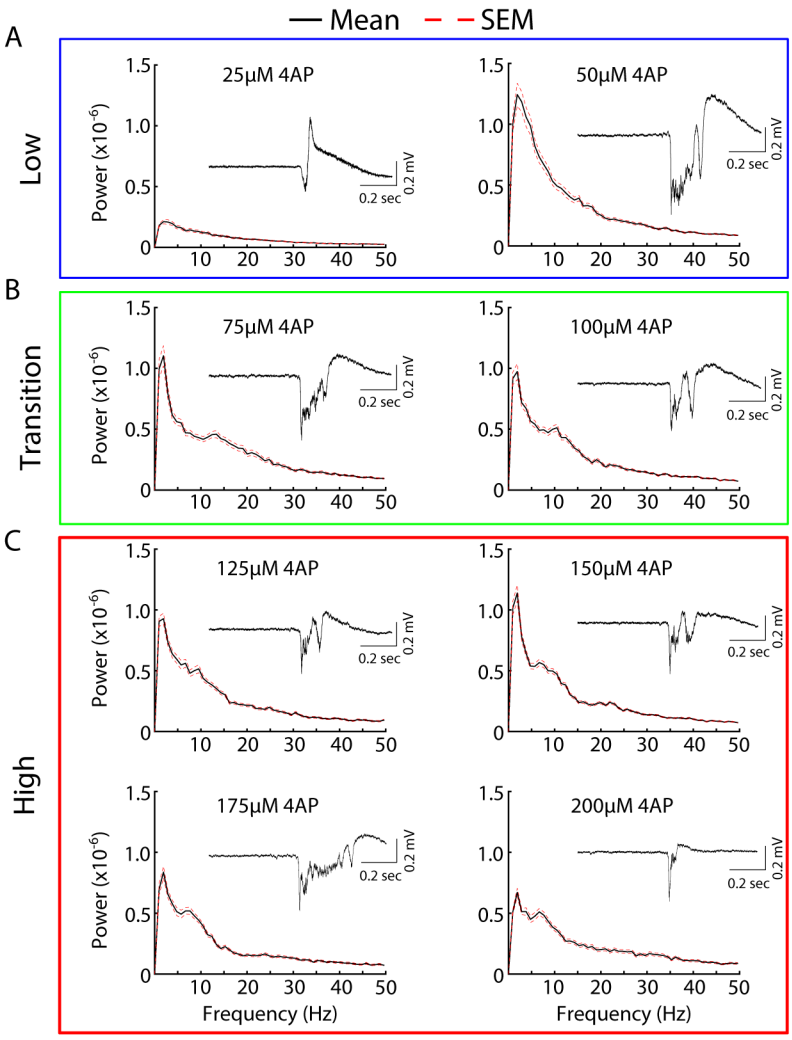

Figure 3:

Concentration-dependent differences in epileptiform spectrograms. Averaged spectrograms of activity induced by different concentrations of 4AP. The mean is plotted in black solid line and standard error (SEM) in red broken line **(A)** Low 4AP concentrations **(B)** Transition concentrations **(C)** High concentrations. Insets are of single representative epileptiform bursts elicited by the corresponding 4AP concentration.

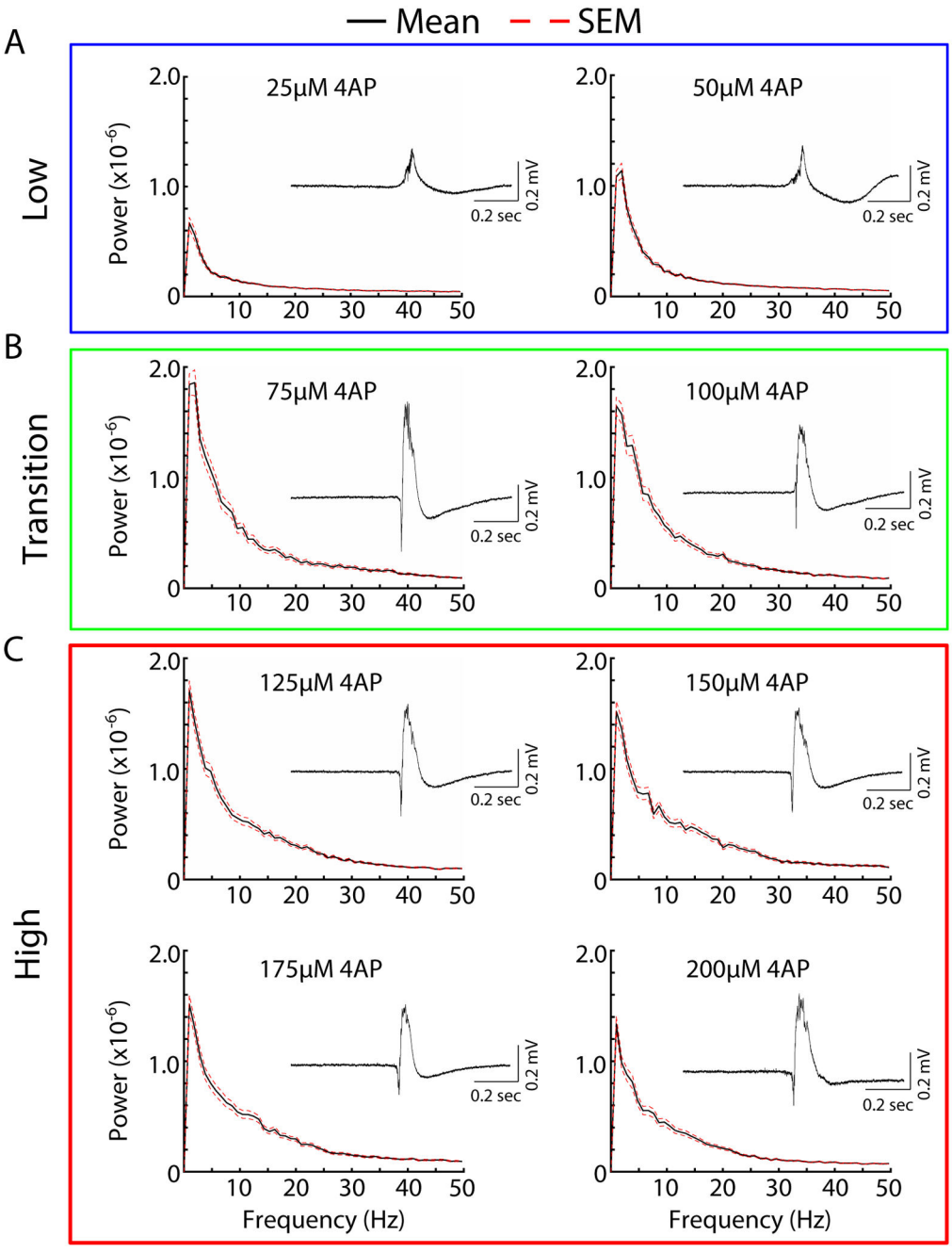

Figure 4: Reduction of KCC2 activity prevents concentration-dependent differences in epileptiform spectrograms.

Averaged spectrograms of activity induced by different concentrations of 4AP and 10 μM VU0240551. The mean is plotted in black solid line and standard error (SEM) in red broken line. **(A)** Low 4AP concentrations **(B)** Transition concentrations **(C)** High concentrations. Insets are of single representative epileptiform bursts elicited by the corresponding 4AP concentration.

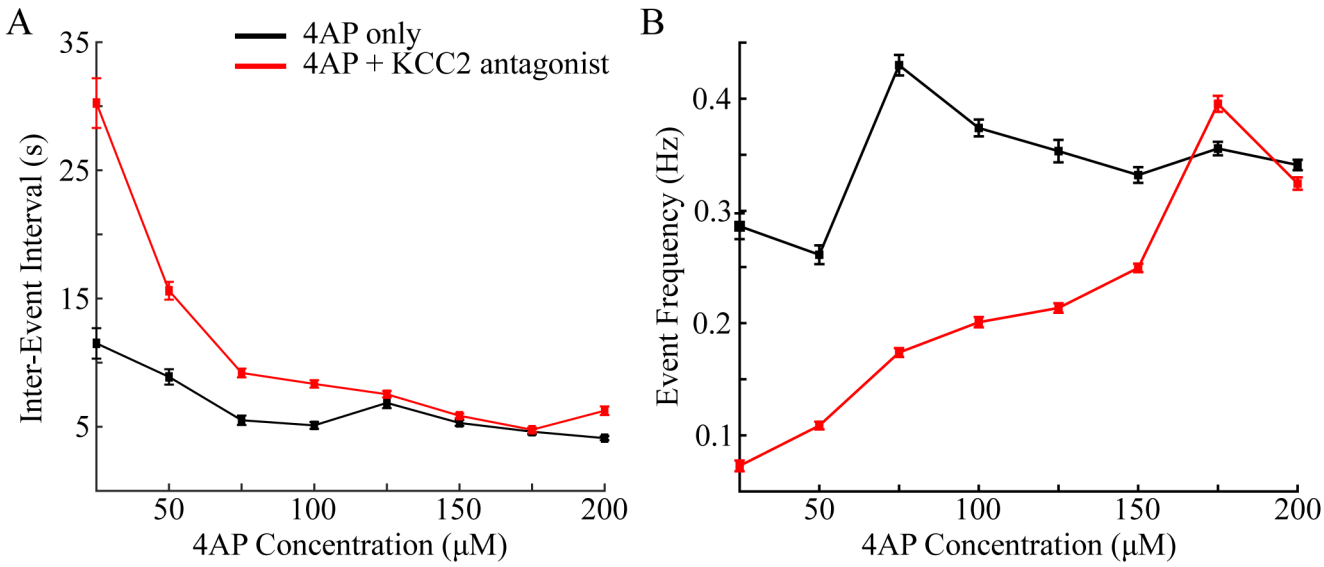

Figure 5:

Differences in inter-event intervals and event frequency of epileptiform bursts. **(A)** Averaged inter-event intervals for difference 4AP concentrations. **(B)** Averaged event frequency of epileptiform bursts per 4AP concentration. Black indicated results for 4AP only, red for 4AP +10 μM VU0240551.

Table 1:

Summary of concentration-dependent effects of 4AP only condition. Numerical values are presented as the mean +/− standard error.

Condition	Low frequency peak	High frequency peak	Inter-event interval	Event frequency
25 μM 4AP	+	−	11.5 s+/−1.187 s	0.2864 Hz +/−0.01152 Hz
50 μM 4AP	+	−	8.887 s+/−0.5993 s	0.2609 Hz +/− 0.008396 Hz
75 μM 4AP	+	+	5.505 s+/−0.3671 s	0.4298 Hz +/− 0.00909 Hz
100 μM 4AP	+	+	5.105 s+/−0.2711 s	0.3739 Hz +/− 0.00747 Hz
125 μM 4AP	+	+	6.862 s+/−0.4185 s	0.3533 Hz +/− 0.009969 Hz
150 μM 4AP	+	+	5.296 s +/− 0.2263 s	0.3319 Hz +/−0.006969 Hz
175 μM 4AP	+	+	4.615 s+/−0.2102 s	0.3556 Hz +/− 0.005989 Hz
200 μM 4AP	+	+	4.110 s+/−0.1629 s	0.3409 Hz +/− 0.004582 Hz

Table 2:

Summary of concentration-dependent effects of 4AP + VU0240551 condition. Numerical values are presented as the mean +/− standard error.

Condition	Low frequency peak	High frequency peak	Inter-event interval	Event frequency
25 μM 4AP + VU0240551	+	−	30.25 s +/− 1.939 s	0.07285 Hz +/− 0.004826 Hz
50 μM 4AP + VU0240551	+	−	15.61 s+/−0.6914 s	0.1087 Hz +/−0.003389 Hz
75 μM 4AP + VU0240551	+	−	9.198 s+/−0.3443 s	0.1738 Hz+/−0.003991 Hz
100 μM 4AP + VU0240551	+	−	8.34 s+/−0.2865 s	0.2008 Hz +/−0.004577 Hz
125 μM 4AP + VU0240551	+	−	7.536 s+/−0.2497 s	0.2135 Hz +/−0.004249 Hz
150 μM 4AP + VU0240551	+	−	5.859 s+/−0.1803 s	0.2492 Hz +/− 0.003724 Hz
175 μM 4AP + VU0240551	+	−	4.764 s+/−0.1667 s	0.3954 Hz +/− 0.0071 Hz
200 μM 4AP + VU0240551	+	−	6.25 s +/− 0.3409 s	0.3244 Hz +/− 0.005448 Hz